



Cite this: *Nanoscale*, 2015, 7, 7022

## Graphene-modified electrodes for enhancing the performance of microbial fuel cells

Heyang Yuan and Zhen He\*

Graphene is an emerging material with superior physical and chemical properties, which can benefit the development of microbial fuel cells (MFC) in several aspects. Graphene-based anodes can enhance MFC performance with increased electron transfer efficiency, higher specific surface area and more active microbe-electrode-electrolyte interaction. For cathodic processes, oxygen reduction reaction is effectively catalyzed by graphene-based materials because of a favorable pathway and an increase in active sites and conductivity. Despite challenges, such as complexity in synthesis and property degeneration, graphene-based electrodes will be promising for developing MFCs and other bioelectrochemical systems to achieve sustainable water/wastewater treatment and bioenergy production.

Received 26th September 2014,  
Accepted 27th October 2014

DOI: 10.1039/c4nr05637j

www.rsc.org/nanoscale

### Introduction

Proper treatment of wastewater is critical to maintain a sustainable society, and this consumes a large amount of energy. For instance, water and wastewater utilities account for approximately 4% of the electricity consumption in the U.S., namely, one third of the total municipal energy budget.<sup>1</sup> It is estimated that the maximal energy that can be extracted from a typical domestic wastewater containing 500 mg L<sup>-1</sup> chemical

oxygen demand (COD) is 1.9 kWh m<sup>-3</sup>.<sup>2</sup> In contrast, approximately 0.6 kWh m<sup>-3</sup> of energy will be consumed to treat this type of domestic wastewater by the prevailing activated sludge method.<sup>3</sup> The theoretical net energy benefit using energy-recovering treatment technology compared to activated sludge methods will be 2.5 kWh m<sup>-3</sup>. Hence, there is an urgent need to develop energy-efficient treatment technologies by reducing energy consumption and increasing energy recovery.

Microbial fuel cell (MFC) as a green treatment technology has attracted considerable attention in the past decade.<sup>4-9</sup> A typical MFC is composed of two electrodes and an ion exchange membrane, which serves as a separator. Organic compounds (e.g. organic wastes in wastewater) are oxidized by

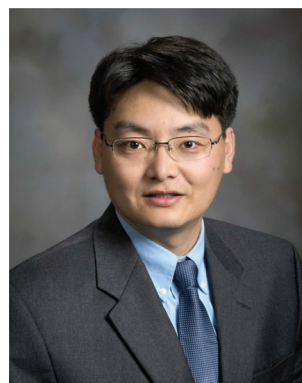
Department of Civil and Environmental Engineering, Virginia Polytechnic Institute and State University, Blacksburg, Virginia 24061, USA. E-mail: zhenhe@vt.edu



Heyang Yuan

Mr Heyang Yuan is now a Ph.D. student advised by Dr Zhen He in the Via Department of Civil and Environmental Engineering at Virginia Polytechnic Institute and State University (Virginia Tech). He received his B.S. from Tongji University and M.S. from Technische Universität München. He has conducted research in microbial communities in activated sludge. At Virginia Tech, his research focuses on electrochemistry in microbial fuel cells,

the optimization of microbial desalination cells, and nano-structured materials for electrode/catalyst application in bioelectrochemical systems



Zhen He

Dr Zhen He is an Associate Professor in the Via Department of Civil and Environmental Engineering at Virginia Tech. Prior to this position, he was an Assistant Professor of Civil Engineering and Mechanics at University of Wisconsin – Milwaukee. He received his BS from Tongji University, MS from Technical University of Denmark, and PhD from Washington University in St. Louis, and all of them were in environmental engineering. His

research focuses on the development of biotechnologies for sustainable water and wastewater treatment. He has published more than 70 journal papers and is an associate editor for *Water Environment Research*.



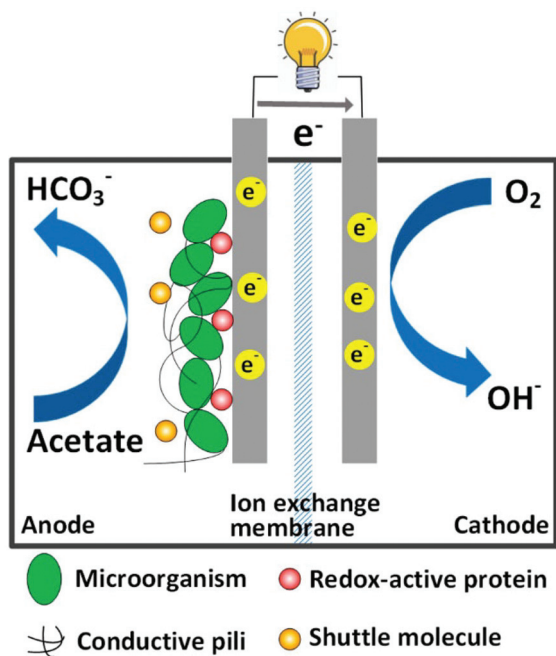


Fig. 1 Schematic of a typical two-chamber MFC.

exoelectrogens (electrochemically active microorganisms) growing on the anode electrode, and terminal electron acceptors (*e.g.* oxygen) are reduced on the cathode electrode (Fig. 1). Because the redox reactions are thermodynamically favorable, electrons released by microorganisms spontaneously flow from the anode electrode to the cathode electrode through an external circuit, and thus electricity is generated.

The development of MFC technology has been hindered mainly by the low charge transfer efficiency of electrodes and high cost of catalysts.<sup>10,11</sup> To address these issues, a variety of materials and their modifications, including carbon/graphite materials, carbon nanotubes (CNTs), nanostructured materials and non-precious metals, have been studied, as reviewed in detail elsewhere.<sup>12,13</sup> While these materials have shown certain promise, their applications are still limited by inherent drawbacks such as low specific surface area, low conductivity, poor biocompatibility, and/or complicated synthesis procedures.

Among these newly developed materials, graphene has been of significant interest since the first demonstration of its facile isolation in 2004.<sup>14</sup> This two-dimensional sheet formed of  $sp^2$  hybridized carbon atoms exhibits outstanding physical properties, including high mechanical strength, high thermal conductivity and good elasticity.<sup>15–17</sup> Its maximal specific surface area is estimated to be  $2630 \text{ m}^2 \text{ g}^{-1}$ , which is several times higher compared to other carbon-based nanomaterials.<sup>18</sup> Furthermore, the superior electrical properties make graphene a promising material for applications in electronics. It has been reported that the charge carrier mobility of suspending single layer graphene can be higher than  $200\,000 \text{ cm}^2 \text{ V}^{-1} \text{ s}^{-1}$ .<sup>19</sup> Consequently, electrons travel in graphene at a Fermi velocity of  $10^6 \text{ m s}^{-1}$  without scattering, which is known as ballistic conduction.<sup>20</sup> These unique properties, which are

tunable towards specific application *via* different synthetic procedures,<sup>21,22</sup> are highly attractive for the development of MFCs. For electrode application, graphene and its modifications may substantially decrease the loss of electrical potential, and thus enhance MFC performance. This review will summarize and discuss graphene-based materials used for MFC application based on their functions, and provide insight into the modification of graphene materials for improving MFC electrodes.

### Enhance the anode performance

Biological oxidation of organics and extracellular electron transfer (EET) are complicated processes affected by several factors. First, electrons are transferred from exoelectrogens to an electrode through three possible mechanisms: (1) soluble electron-shuttling molecules, (2) redox-active proteins on the cell membrane and (3) conductive pili.<sup>23</sup> Therefore, an ideal anode electrode is expected to facilitate rapid heterogeneous electron transfer (HET) with microorganisms and electron shuttles.<sup>24</sup> Moreover, a bioanode should have biocompatibility and a high specific surface area for accommodating a large quantity of microbes. In this regard, graphene-based materials are promising candidates for highly efficient MFC anodes.<sup>25,26</sup> The following sections discuss the study of graphene-based materials in MFC anodes from the aspects of EET efficiency, specific surface area and multi-phase interactions.

### Improving EET efficiency

It has been determined that graphene-based materials could improve EET efficiency through functional groups. In an early MFC study that involved graphene-based materials, graphene oxide (GO), a common precursor in graphene synthesis, was examined as an anode.<sup>27</sup> Cyclic voltammetry (CV) results suggested that the GO nanoribbons yielded a higher response of cytochromes (redox-active proteins), indicating lower activation energy, namely, a lower potential loss. This finding is unexpected because GO is considered as an insulator and only shows graphene-like conductivity after being reduced.<sup>28</sup> Thus, researchers attributed the enhanced electrochemical activity to the large amount of functional groups on the material surface. The properties of GO were further studied by forming a polypyrrole/GO composite, which was designed to take advantage of the conductivity of polypyrrole and the electrochemical activity of functional groups from GO.<sup>29</sup> As anticipated, the composite achieved a noticeably higher power density compared to reduced GO and pristine polypyrrole. Electrochemical impedance spectroscopy (EIS) also revealed a slight reduction in the ohmic resistance and a significant decrease in the charge transfer resistance.

With advances in materials science, graphene is easily obtained by the reduction of GO.<sup>30</sup> As a consequence, anode electrodes modified with graphene materials through various methods have been investigated for MFCs. The most straightforward method is to directly coat graphene on anode electrodes, *e.g.* on stainless steel fiber felts. In comparison to activated carbon and CNTs, graphene-coated anode exhibited remarkably high electrochemical response in CV and the



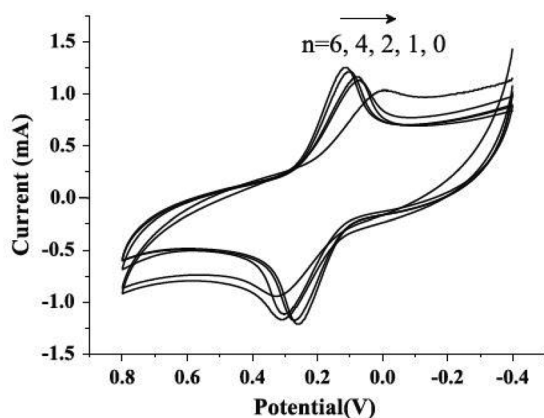


Fig. 2 Cyclic voltammograms of  $n$ -layer graphene composites ( $n = 0, 1, 2, 4, 6$ ) in aqueous  $0.1 \text{ mol L}^{-1}$  KCl containing  $10 \text{ mmol L}^{-1}$   $\text{K}_3[\text{Fe}(\text{CN})_6]$  at a scan rate of  $20 \text{ mV s}^{-1}$ . Reproduction with permission from ref. 32.

lowest polarization resistance. Although the charge transfer resistance of graphene anode was higher compared to CNT anode, suggesting a relatively inferior HET, it still provided the highest power density among the tested electrodes.<sup>31</sup> To enhance HET, Guo *et al.*<sup>32</sup> modified carbon paper with graphene *via* layer-by-layer assembly and observed increased peak current and decreased peak current separation in CV when the layer number increased (Fig. 2). These results clearly evidenced a promoted electron transfer rate and were further supported by the same trend of charge transfer resistance in EIS tests. Charge transfer resistance was also successfully reduced together with a boosted peak current when tin oxide was anchored on the surface of reduced GO (rGO) using a microwave-assisted method.<sup>32</sup>

An interesting phenomenon, which can be directly related to both EET and GO reduction, is that GO can be *in situ* reduced *via* the respiration of bacteria such as *Shewanella* spp.,<sup>33</sup> which is a group of important facultative exoelectrogens in MFCs.<sup>34</sup> Electron transfer during the microbial reduction on graphene has been reported to be involved with cytochromes *MtrA*, *MtrB*, and *MtrC/OmcA*, which are all playing pivotal roles in EET.<sup>35</sup> This has raised the question if biologically reduced GO interacts better with microbes and shows higher EET efficiency. A further study using microbiologically reduced GO as an anode material demonstrated a 25-fold higher electron transfer rate constant, doubled exchange current and halved ohmic and charge transfer resistance.<sup>36</sup> Distinct improvement of these properties is encouraging for the development of highly robust and sustainable anode electrodes *via in situ* reduction in MFCs.

### Increasing specific surface area

A high specific surface area of graphene can provide sufficient sites for the attachment of biofilms, and consequently guarantee a high quantity of biocatalysts for the oxidation of organics.<sup>37</sup> For example, the specific surface area of graphene obtained *via* chemical reduction is 500 times larger compared

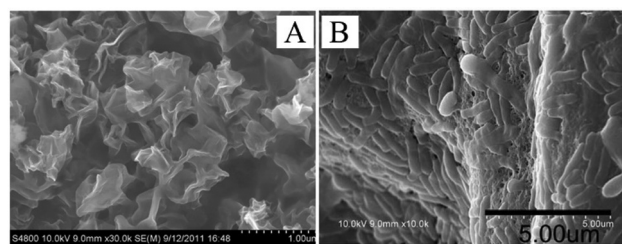


Fig. 3 (A) Morphology of crumpled r-GO particles. (B) SEM images of the attachment of bacterial cells on the graphene/PANI anodes. Reproduction with permission from ref. 42, 43.

to woven graphite felt.<sup>38,39</sup> However, this specific surface area is only one tenth of the theoretical value, indicating a reduction in area caused by increased layer number or other treatments.<sup>21,40</sup> To fully exploit this advantage of graphene materials, modifications were carried out from different aspects. Luo *et al.*<sup>41</sup> introduced an evaporation-induced crumpling process to synthesize compression- and aggregation-resistant graphene balls, which yielded crumpled graphene particles with a specific surface area up to  $567 \text{ m}^2 \text{ g}^{-1}$ . Electricity generation and power density of the MFC equipped with the crumpled graphene anode (Fig. 3A) was significantly enhanced compared to regular graphene sheets.<sup>42</sup>

Polyaniline (PANI) was electro-deposited on graphene nanoribbons to fabricate a composite anode, as this polymer has been reported to easily form porous nanostructures.<sup>43</sup> Scanning electron microscopy (SEM) results demonstrated a 3D microporous structure and dense adhesion of microbial cells on the anode surface. As a result of the thickened biofilm (Fig. 3B), the PANI/graphene-anode MFC produced a maximal power density twice as high as that of the control group. Later, a simple synthesis of macroporous 3D graphene sponge was developed by freeze-drying frozen graphene hydrogel.<sup>44</sup> A noticeable increase in both specific surface area and pore volume was observed. It could also be seen from SEM images that organisms thrived on a graphene anode, which was in good agreement with the increased power density.

### Promoting interaction among microbes, substrates and electrodes

Although the biocompatibility of graphene remains inconclusive,<sup>30</sup> graphene anodes have been reported to change microbial metabolism in a manner that favors EET. For example, Liu *et al.*<sup>45</sup> obtained high peak current and lower peak separation when using a graphene-deposited carbon cloth anode. As discussed earlier, these results indicated a facilitated EET. Interestingly, when peak current was plotted *versus* square root of scan rate or scan rate, which represented mediated and direct electron transfer, respectively, it was observed that the positive effect exerted by graphene anode was more significant to direct EET compared to mediated EET (Fig. 4). This finding, together with a high amount of biomass observed on the anode surface, may be indicative that exoelectrogens integrated graphene materials into their EET pathways.



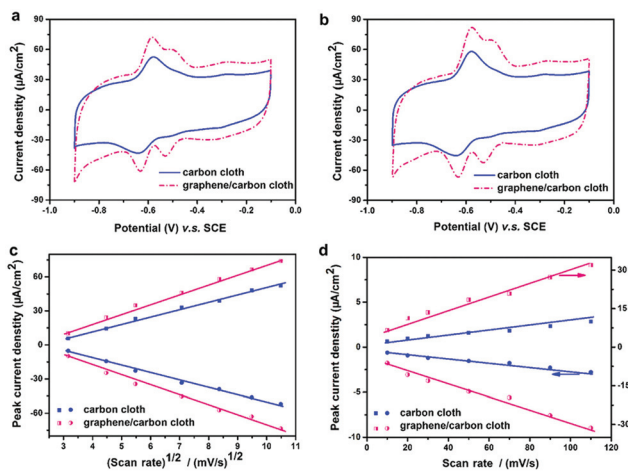


**Fig. 4** (A) Cyclic voltammograms of MFC in glucose-free medium and (B) in 0.5% glucose medium at a scan rate of  $30 \text{ mV s}^{-1}$ . (C) Peak current of Peak 1 ( $-0.6 \text{ V vs. SCE}$ ) is plotted versus the square root of scan rate. (D) Peak current of Peak 2 ( $-0.5 \text{ V vs. SCE}$ ) is plotted versus scan rate. Reproduction with permission from ref. 45.

A similar conclusion was drawn in a recent study,<sup>46</sup> in which CV response associated with outer membrane *c*-type cytochrome was detected on a microbiologically reduced graphene/Shewanella biofilm but not on a pristine biofilm, indicating a highly integrated microbe/electrode hybrid. Furthermore, the 3D macroporous structure of the resultant composite ensured good interaction between biocatalyst and substrate.<sup>46</sup> It is noteworthy that the enhancement of conductive pili, which is one of the major electron transfer mechanisms, has by far not been reported. Hypothetically, the biocompatibility and porous structure of graphene-based electrode may be favorable for the formation of conductive pili, further facilitating microbe-electrode interaction. Understanding the effects of graphene materials on the pili formation may significantly advance graphene application as bio-electrode materials in MFC.

In addition to creating a porous structure, PANI is positively charged in neutral solutions, and thus shows high affinity towards the negatively charged biomass.<sup>47</sup> Moreover, biofilm formation on the hydrophobic graphene is expected to be improved with the hydrophilic PANI.<sup>48</sup> In a recent study, CV peak related to a *c*-type cytochrome (presumably *OmcA*) was detected using a PANI-hybridized 3D graphene anode, but was absent for carbon cloth anode.<sup>49</sup> Furthermore, high performance liquid chromatography did not detect difference in the concentrations of riboflavin, a relevant electron shuttle, between the MFCs equipped with those two anodes. Therefore, it was concluded that electrons were preferentially harvested *via* direct EET on the graphene/PANI anode due to its 3D integration with biofilm. Hou *et al.*<sup>50</sup> obtained reduced graphene *via* electrochemical reduction and mixed it with PANI to fabricate MFC anodes. Although the PANI-rGO anode showed slightly higher charge transfer resistance compared to pristine reduced graphene anode, its power density and open circuit voltage outperformed other materials. It is noteworthy that in

the two studies, the diffusion resistance of the PANI-modified graphene was significantly smaller compared to non-modified graphene or other materials, indicating a favorable structure for the interaction between electrolyte and anode electrode.

### Enhance the cathode

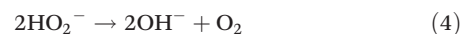
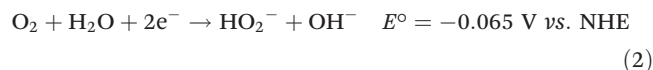
Oxygen is an ideal electron acceptor for MFC cathode because of its reduction potential and availability. However, the reduction of oxygen is kinetically slow, and hence may contribute to the internal resistance of an MFC more than anode reaction.<sup>51</sup> In addition, oxygen reduction reaction (ORR) occurring at the cathode surface involves three phases, *i.e.*, gas (oxygen-electron acceptor), liquid (electrolyte-reaction medium) and solid (electrode-electron donor), making it a complicated process. As such, the cathode process is considered to be challenging and requires efficient catalysts (*e.g.* simple synthesis and cost effective catalysis) to facilitate ORR.<sup>11</sup> Platinum (Pt) is commonly used as a catalyst in bench-scale MFC experiments owing to the small overpotential of ORR, but Pt-based catalysts are not economically viable in large-scale applications, especially for wastewater treatment. A number of carbon-based materials and non-precious metals have been intensively studied as alternative materials for cathode electrodes and catalysts in the past few years, and there is a continuing interest in exploring more efficient catalysts to improve the cathode performance.<sup>13</sup> Graphene modification has been demonstrated to be effective to carry out ORR *via* an efficient pathway (*i.e.* four-electron transfer), abundant active sites and high conductivity.<sup>52</sup>

### Cathode reduction pathways

In principle, oxygen is reduced either through a one-step four-electron pathway (eqn (1)):



or a less efficient two-electron pathway (eqn (2)), followed by the reduction of  $\text{HO}_2^-$  (eqn (3)) or by the more rapid disproportionation of  $\text{HO}_2^-$  (eqn (4)).<sup>53,54</sup>



While the 2-e pathway generates highly reactive hydrogen peroxide, which leads to damaged membranes and electrodes, the 4-e pathway is favorable because of the higher reduction potential. It has been determined that four-electron transfer predominates in ORR using nitrogen-doped graphene (NG) as a cathode material.<sup>55</sup> The transferred electron number per oxygen molecule was calculated to be 3.69 for a NG cathode synthesized with detonation process, close to that for Pt. In another study, NG obtained *via* pyrolysis yielded an even higher electron transfer number of 3.87.<sup>56</sup> Both studies achieved slightly higher power density with NG cathode com-



pared with Pt in MFCs. The superior ORR catalysis is mainly attributed to the introduction of three nitrogen species by doping: graphitic N adsorbs OOH and reduces  $O_2$  to  $H_2O_2$  via 2-e pathway, and pyridinic and pyrrolic N are likely to be responsible for the catalysis of 4-e pathway.<sup>56–59</sup>

According to Cao *et al.*,<sup>60</sup> ORR can be catalyzed by manganese oxides possibly through the oxidation of MnOOH by adsorbed oxygen. As demonstrated by CV, ORR catalysis by  $MnO_2$  coated on graphene was significantly enhanced compared with that on carbon black and multi-wall CNT (MWCNT).<sup>61</sup> Moreover, the performance of the MFC equipped with  $MnO_2$ /graphene cathode was comparable to that with Pt/C in terms of open circuit voltage, power density and coulombic efficiency. A  $MnO_2$ /GO cathode also provided power density and electricity generation similar to that of a Pt/C cathode.<sup>62</sup> Graphene electrodes hybridized with other metals resulted in similar enhancement in the MFC performance.<sup>63–66</sup> These studies suggest that graphene can affect ORR pathway either by the modification of its own structure or by the enhancement of catalytic ability with other doped/coated materials.

### Increasing active sites

As discussed above, a high content of pyridinic and pyrrolic nitrogen in NG is desirable because they might facilitate the more efficient four-electron transfer in ORR. To increase the proportion of these nitrogen active sites, Feng *et al.*<sup>67</sup> implanted mesoporous graphitic carbon nitride ( $C_3N_4$ ) into NG nanosheet. This novel approach resulted in a high nitrogen/carbon ratio of 19.7% and an increased content of pyridinic N, which is distinctly higher than that synthesized using pyrrole, aniline and ammonia as precursors.<sup>57</sup> The remarkable ORR catalysis of the implanted NG was later testified by electrochemical analysis, in which CV showed a higher peak current, whereas linear sweep voltammetry provided an earlier onset potential compared to Pt/C. Furthermore, the transferred electron number was calculated to be 4, indicating a complete four-electron transfer pathway.<sup>67</sup> When tested in MFCs, the modified NG yielded 20% higher power density (Fig. 5A) and noticeably higher stability compared to Pt/C (Fig. 5B). The increase in nitrogen activity can also be implemented from other aspects. For example, iron was added to stabilize nitrogen incorporation on graphene.<sup>68</sup>

In addition to the amount of nitrogen sites, sufficient exposure of active sites to reactants using a large specific surface area could effectively promote ORR. PANI was hybridized with GO to produce porous nitrogen-doped carbon nanosheet on graphene with a specific surface area of  $1398\text{ m}^2\text{ g}^{-1}$ , leading to a prominent CV peak and power density.<sup>69</sup> In the same study, oxygen content in the modified material reached a high value of 9.13%, which could be another explanation for the efficient catalysis. Oxygen species were also observed in  $C_3N_4$ -NG, which was speculated to be advantageous to ORR because of the high adsorption of  $O_2$ .<sup>70</sup> Liu *et al.*<sup>56</sup> has proposed that the presence of O species not only decreases the active energy carrier of ORR, but also protects the catalytic C-N groups from being attacked by protons

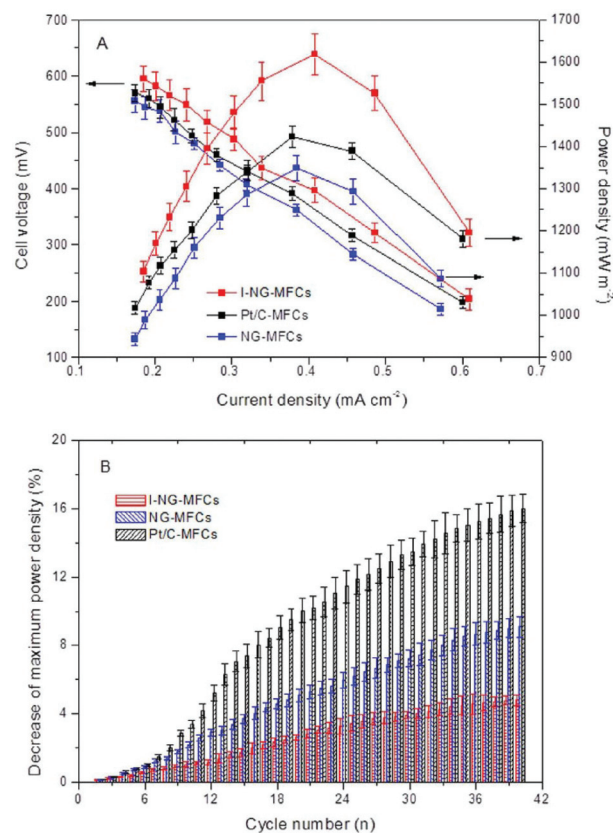


Fig. 5 (A) Power densities and cell voltages of mesoporous graphitic  $C_3N_4$ -NG MFCs, regular NG-MFCs and Pt/C-MFCs. (B) Reduction of maximum power density with cycle number at an external resistance of  $1000\ \Omega$ . Reproduction with permission from ref. 67.

(Fig. 6). Apart from oxygen, other polar functional groups on the graphene surface have been reported to encourage the formation of small silver particles, whose size is inversely correlated to ORR catalysis, resulting in an electron transfer number of 3.8 and comparable power density and electricity generation to Pt/C.<sup>71</sup>

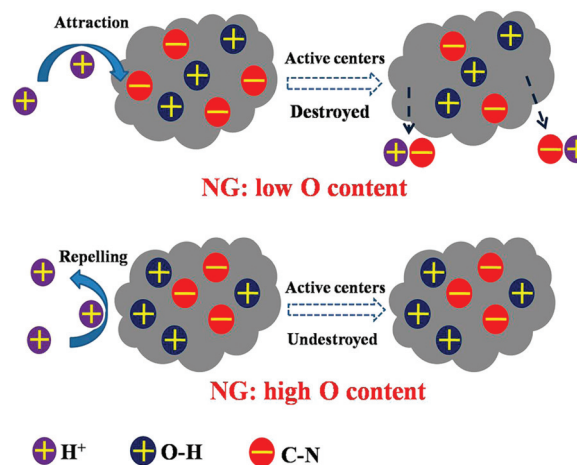


Fig. 6 NG is protected by O-H groups from the attack of protons. Reproduction with permission from ref. 56.



## Enhancing conductivity

Although in theory graphene possesses high conductivity, non-ballistic conduction was observed in bulk samples,<sup>72</sup> possibly resulted from impurity and topological lattice defects.<sup>21,73,74</sup> This increases the internal resistance of the cathode electrode, and thus hinders ORR. Therefore, it is of crucial importance to maximize the conductivity of graphene cathodes in practical applications. To reduce resistance, graphene is doped with nitrogen. The conductivity of regular NG was measured to be 35 S m<sup>-1</sup>, which is 10 S m<sup>-1</sup> lower compared to Pt/C,<sup>55</sup> whereas that of C<sub>3</sub>N<sub>4</sub>-implanted NG increased to 66 S m<sup>-1</sup>.<sup>67</sup> Accordingly, the MFC with an implanted NG cathode, which showed a 31% decrease of internal resistance, produced a 20% higher power density compared to the one with a regular NG cathode. Similar to graphene-based anode electrodes, the ohmic and charge transfer resistance of cathode electrodes can be reduced with graphene/biofilm composites or crumpled graphene particles.<sup>42,75</sup> The versatile polymer PANI has also been doped with graphene to fabricate cathode electrodes.<sup>76</sup> EIS results revealed the diminished ohmic and charge transfer resistance for the PANI-graphene cathodes compared to the pristine PANI cathode, with the PANI/graphene ratio of 1:9 being the most conductive electrode. The PANI/graphene composites doped with *para*-toluenesulfonic acid exhibited high electrical conductivity at high temperature due to the high mobility of the charge carriers.<sup>77</sup>

## Perspectives

It is worth noting that in most cases, the enhanced performance of anode electrodes and/or cathode electrodes, conferred by graphene materials, is a synergistic effect.<sup>78–81</sup> For example, a chitosan/vacuum-stripped graphene scaffold composite with hierarchically porous 3D structure had a specific surface area of 248 m<sup>2</sup> g<sup>-1</sup> owing to the large specific areas of graphene.<sup>82</sup> Moreover, its charge transfer resistance was reduced with increased graphene loading, with the lowest value of 150 Ω for 50 wt% among a series of loading rates. Together with the good biofilm adhesion and high production of endogenous mediator stimulated by the biocompatible chitosan, current and power density of the MFC containing this composite as its anode electrode were 16 and 78 times higher, respectively, compared to the control with the carbon cloth anode. On the other hand, multi-directional improvement was also observed in cathode modifications, for example implantation of mesoporous graphitic C<sub>3</sub>N<sub>4</sub> simultaneously facilitated favorable ORR pathway and increased active sites and conductivity.<sup>67</sup> Therefore, synergistic effects are desirable as electrode performance benefited from multiplication instead of addition of the enhancement of individual aspects. This may be helpful for the preparation and modification of graphene-based electrode and catalysts in future.

Despite their great promise in MFCs, graphene materials suffer from relatively complicated synthesis procedures. In general, graphene electrodes are prepared through three steps: GO synthesis, GO reduction to graphene, and modification.<sup>83</sup>

This approach, and other methods, including chemical vapor deposition,<sup>84</sup> unzipping of MWCNTs and detonation are either troublesome, energy/time-consuming or involved with hazardous chemicals,<sup>27,49,55</sup> thereby increasing capital cost in large-scale applications. The *in situ* reduction of GO to graphene by bacteria or phytoextracts could be an effective option for anode fabrication as it meets the requirement of sustainability and green chemistry.<sup>85</sup> For cathode, NG is a competitive material because of its outstanding ORR catalysis, but does not seem to prevail before economic synthesis methods with optimized nitrogen types and contents are developed.<sup>59</sup>

MFCs are a major type of bioelectrochemical systems (BES), which also include various ramifications with different functions such as the hydrogen-producing microbial electrolysis cells (MECs), the chemical-synthesizing microbial synthesis cells (MSCs) and the salt-removing microbial desalination cells.<sup>4</sup> To date, there is very limited study using graphene to enhance performance in BES other than MFCs.<sup>86</sup> In a study of MECs, 3D MoS<sub>2</sub>/NG nanosheet aerogels were synthesized through a facile hydrothermal approach and used to catalyze hydrogen evolution reaction (HER). Although the loading rate of MoS<sub>2</sub>/NG aerogels on the cathode electrode was only 25% that of Pt/C, its current density in MFC test was comparable to that of Pt/C. In addition, the MoS<sub>2</sub>/NG aerogels outperformed pristine MoS<sub>2</sub> nanosheets and NG aerogels with respect to electrochemistry and catalysis. It can be expected that with advances in graphene research, there will be more research using graphene materials as electrode and catalyst for improving BES performance in a broad range of applications, and in return this will be beneficial for identifying proper application niches for graphene materials and stimulating graphene research in future.

## Acknowledgements

The authors acknowledge the financial support from a faculty startup fund of Virginia Polytechnic Institute and State University.

## Notes and references

- 1 R. Goldstein and W. Smith, *Water & Sustainability (Volume 4): US Electricity Consumption for Water Supply & Treatment-The Next Half Century*, Electric Power Research Institute, 2002.
- 2 P. L. McCarty, J. Bae and J. Kim, *Environ. Sci. Technol.*, 2011, **45**, 7100–7106.
- 3 T. P. Curtis, *Environ. Microbiol.*, 2010, **2**, 301–318.
- 4 H. Wang and Z. J. Ren, *Biotechnol. Adv.*, 2013, **31**, 1796–1807.
- 5 W.-W. Li, H.-. Yu and Z. He, *Energy Environ. Sci.*, 2013, **7**, 911–924.



- 6 V. B. Wang, N. Yantara, T. M. Koh, S. Kjelleberg, Q. Zhang, G. C. Bazan, S. C. J. Loo and N. Mathews, *Chem. Commun.*, 2014, **50**, 8223–8226.
- 7 V. B. Wang, S.-L. Chua, Z. Cai, K. Sivakumar, Q. Zhang, S. Kjelleberg, B. Cao, S. C. J. Loo and L. Yang, *Bioresour. Technol.*, 2014, **155**, 71–76.
- 8 V. B. Wang, N. D. Kirchofer, X. Chen, M. Y. L. Tan, K. Sivakumar, B. Cao, Q. Zhang, S. Kjelleberg, G. C. Bazan, S. C. J. Loo and E. Marsili, *Electrochem. Commun.*, 2014, **41**, 55–58.
- 9 V. B. Wang, J. Du, X. Chen, A. W. Thomas, N. D. Kirchofer, L. E. Garner, M. T. Maw, W. H. Poh, J. Hinks, S. Wuertz, S. Kjelleberg, Q. Zhang, J. S. C. Loo and G. C. Bazan, *Phys. Chem. Chem. Phys.*, 2013, **15**, 5867–5872.
- 10 R. A. Rozendal, H. V. Hamelers, K. Rabaey, J. Keller and C. J. Buisman, *Trends Biotechnol.*, 2008, **26**, 450–459.
- 11 B. E. Logan, *Appl. Microbiol. Biotechnol.*, 2010, **85**, 1665–1671.
- 12 Y. Qiao, S.-J. Bao and C. M. Li, *Energy Environ. Sci.*, 2010, **3**, 544–553.
- 13 M. Zhou, M. Chi, J. Luo, H. He and T. Jin, *J. Power Sources*, 2011, **196**, 4427–4435.
- 14 K. S. Novoselov, A. K. Geim, S. Morozov, D. Jiang, Y. Zhang, S. Dubonos, I. Grigorieva and A. Firsov, *Science*, 2004, **306**, 666–669.
- 15 C. Lee, X. Wei, J. W. Kysar and J. Hone, *Science*, 2008, **321**, 385–388.
- 16 A. A. Balandin, S. Ghosh, W. Bao, I. Calizo, D. Teweldebrhan, F. Miao and C. N. Lau, *Nano Lett.*, 2008, **8**, 902–907.
- 17 K. S. Kim, Y. Zhao, H. Jang, S. Y. Lee, J. M. Kim, K. S. Kim, J.-H. Ahn, P. Kim, J.-Y. Choi and B. H. Hong, *Nature*, 2009, **457**, 706–710.
- 18 M. D. Stoller, S. Park, Y. Zhu, J. An and R. S. Ruoff, *Nano Lett.*, 2008, **8**, 3498–3502.
- 19 K. I. Bolotin, K. J. Sikes, Z. Jiang, M. Klima, G. Fudenberg, J. Hone, P. Kim and H. L. Stormer, *Solid State Commun.*, 2008, **146**, 351–355.
- 20 X. Du, I. Skachko, A. Barker and E. Y. Andrei, *Nat. Nanotechnol.*, 2008, **3**, 491–495.
- 21 R. S. Edwards and K. S. Coleman, *Nanoscale*, 2013, **5**, 38–51.
- 22 X. Huang, Z. Yin, S. Wu, X. Qi, Q. He, Q. Zhang, Q. Yan, F. Boey and H. Zhang, *Small*, 2011, **7**, 1876–1902.
- 23 D. R. Lovley, *Annu. Rev. Microbiol.*, 2012, **66**, 391–409.
- 24 F. Zhao, R. C. Slade and J. R. Varcoe, *Chem. Soc. Rev.*, 2009, **38**, 1926–1939.
- 25 C. Zhao, Y. Wang, F. Shi, J. Zhang and J.-J. Zhu, *Chem. Commun.*, 2013, **49**, 6668–6670.
- 26 Y. Zhu, J. Ji, J. Ren, C. Yao and L. Ge, *Colloids Surf., A*, 2014, **455**, 92–96.
- 27 Y.-X. Huang, X.-W. Liu, J.-F. Xie, G.-P. Sheng, G.-Y. Wang, Y.-Y. Zhang, A.-W. Xu and H.-Q. Yu, *Chem. Commun.*, 2011, **47**, 5795–5797.
- 28 K. P. Loh, Q. Bao, G. Eda and M. Chhowalla, *Nat. Chem.*, 2010, **2**, 1015–1024.
- 29 Z. Lv, Y. Chen, H. Wei, F. Li, Y. Hu, C. Wei and C. Feng, *Electrochim. Acta*, 2013, **111**, 366–373.
- 30 J. Filip and J. Tkac, *Electrochim. Acta*, 2014, **136**, 340–354.
- 31 J. Hou, Z. Liu, S. Yang and Y. Zhou, *J. Power Sources*, 2014, **258**, 204–209.
- 32 W. Guo, Y. Cui, H. Song and J. Sun, *Bioprocess Biosyst. Eng.*, 2014, **37**, 1749–1758.
- 33 G. Wang, F. Qian, C. Saltikov, Y. Jiao and Y. Li, *Nano Res.*, 2011, **4**, 563–570.
- 34 E. C. Salas, Z. Sun, A. Lüttge and J. M. Tour, *ACS Nano*, 2010, **4**, 4852–4856.
- 35 S. Patil, C. Hägerhäll and L. Gorton, *Bioanal. Rev.*, 2012, **4**, 159–192.
- 36 Y. Yuan, S. Zhou, B. Zhao, L. Zhuang and Y. Wang, *Bioresour. Technol.*, 2012, **116**, 453–458.
- 37 A. Mehdinia, E. Ziaei and A. Jabbari, *Int. J. Hydrogen Energy*, 2014, **39**, 10724–10730.
- 38 D. H. Park and J. G. Zeikus, *Biotechnol. Bioeng.*, 2003, **81**, 348–355.
- 39 Y. Zhang, G. Mo, X. Li, W. Zhang, J. Zhang, J. Ye, X. Huang and C. Yu, *J. Power Sources*, 2011, **196**, 5402–5407.
- 40 H. Skulason, P. Gaskell and T. Szkopek, *Nanotechnology*, 2010, **21**, 295709.
- 41 J. Luo, H. D. Jang, T. Sun, L. Xiao, Z. He, A. P. Katsoulidis, M. G. Kanatzidis, J. M. Gibson and J. Huang, *ACS Nano*, 2011, **5**, 8943–8949.
- 42 L. Xiao, J. Damien, J. Luo, H. D. Jang, J. Huang and Z. He, *J. Power Sources*, 2012, **208**, 187–192.
- 43 C. Zhao, P. Gai, C. Liu, X. Wang, H. Xu, J. Zhang and J.-J. Zhu, *J. Mater. Chem. A*, 2013, **1**, 12587–12594.
- 44 W. Chen, Y.-X. Huang, D.-B. Li, H.-Q. Yu and L. Yan, *RSC Adv.*, 2014, **4**, 21619–21624.
- 45 J. Liu, Y. Qiao, C. X. Guo, S. Lim, H. Song and C. M. Li, *Bioresour. Technol.*, 2012, **114**, 275–280.
- 46 Y.-C. Yong, Y.-Y. Yu, X. Zhang and H. Song, *Angew. Chem., Int. Ed.*, 2014, **53**, 4480–4483.
- 47 B. Lai, X. Tang, H. Li, Z. Du, X. Liu and Q. Zhang, *Biosens. Bioelectron.*, 2011, **28**, 373–377.
- 48 P. Avouris and C. Dimitrakopoulos, *Mater. Today*, 2012, **15**, 86–97.
- 49 Y.-C. Yong, X.-C. Dong, M. B. Chan-Park, H. Song and P. Chen, *ACS Nano*, 2012, **6**, 2394–2400.
- 50 J. Hou, Z. Liu and P. Zhang, *J. Power Sources*, 2013, **224**, 139–144.
- 51 Y. Fan, E. Sharbrough and H. Liu, *Environ. Sci. Technol.*, 2008, **42**, 8101–8107.
- 52 Y. Zhang, G. Mo, X. Li and J. Ye, *J. Power Sources*, 2012, **197**, 93–96.
- 53 A. J. Bard and L. R. Faulkner, *Electrochemical methods: fundamentals and applications*, Wiley, New York, 1980.
- 54 S. Maldonado and K. J. Stevenson, *J. Phys. Chem. B*, 2005, **109**, 4707–4716.
- 55 L. Feng, Y. Chen and L. Chen, *ACS Nano*, 2011, **5**, 9611–9618.
- 56 Y. Liu, H. Liu, C. Wang, S.-X. Hou and N. Yang, *Environ. Sci. Technol.*, 2013, **47**, 13889–13895.



- 57 L. Lai, J. R. Potts, D. Zhan, L. Wang, C. K. Poh, C. Tang, H. Gong, Z. Shen, J. Lin and R. S. Ruoff, *Energy Environ. Sci.*, 2012, **5**, 7936–7942.
- 58 K. Gong, F. Du, Z. Xia, M. Durstock and L. Dai, *Science*, 2009, **323**, 760–764.
- 59 H. Wang, T. Maiyalagan and X. Wang, *ACS Catal.*, 2012, **2**, 781–794.
- 60 Y. L. Cao, H. X. Yang, X. P. Ai and L. F. Xiao, *J. Electroanal. Chem.*, 2003, **557**, 127–134.
- 61 S. Khilari, S. Pandit, M. M. Ghangrekar, D. Das and D. Pradhan, *RSC Adv.*, 2013, **3**, 7902–7911.
- 62 G. Gnana kumar, Z. Awan, K. Suk Nahm and J. Stanley Xavier, *Biosens. Bioelectron.*, 2014, **53**, 528–534.
- 63 G. H. Qi, X. Q. Li and J. Cao, *Adv. Mater. Res.*, 2014, **881**, 310–314.
- 64 Q. Wen, S. Wang, J. Yan, L. Cong, Z. Pan, Y. Ren and Z. Fan, *J. Power Sources*, 2012, **216**, 187–191.
- 65 Z. Yan, M. Wang, B. Huang, R. Liu and J. Zhao, *Int. J. Electrochem. Sci.*, 2013, **8**, 149–158.
- 66 Y. Su, Y. Zhu, X. Yang, J. Shen, J. Lu, X. Zhang, J. Chen and C. Li, *Ind. Eng. Chem. Res.*, 2013, **52**, 6076–6082.
- 67 L. Feng, L. Yang, Z. Huang, J. Luo, M. Li, D. Wang and Y. Chen, *Sci. Rep.*, 2013, **3**.
- 68 S. Li, Y. Hu, Q. Xu, J. Sun, B. Hou and Y. Zhang, *J. Power Sources*, 2012, **213**, 265–269.
- 69 Q. Wen, S. Wang, J. Yan, L. Cong, Y. Chen and H. Xi, *Bioelectrochemistry*, 2014, **95**, 23–28.
- 70 P. G. Collins, K. Bradley, M. Ishigami and A. Zettl, *Science*, 2000, **287**, 1801–1804.
- 71 S. Hongliang, X. Kongliang, L. Guolong, L. Hongbin and L. Zhenning, *IEEE Trans. Nanotechnol.*, 2014, **13**, 789–794.
- 72 F. Miao, S. Wijeratne, Y. Zhang, U. C. Coskun, W. Bao and C. N. Lau, *Science*, 2007, **317**, 1530–1533.
- 73 A. M. Ilyin, E. A. Daineko and G. W. Beall, *Physica E*, 2009, **42**, 67–69.
- 74 S. Adam, E. H. Hwang, E. Rossi and S. Das Sarma, *Solid State Commun.*, 2009, **149**, 1072–1079.
- 75 L. Zhuang, Y. Yuan, G. Yang and S. Zhou, *Electrochem. Commun.*, 2012, **21**, 69–72.
- 76 Y. Ren, D. Pan, X. Li, F. Fu, Y. Zhao and X. Wang, *J. Chem. Technol. Biotechnol.*, 2013, **88**, 1946–1950.
- 77 M. O. Ansari, M. M. Khan, S. A. Ansari, I. Amal, J. Lee and M. H. Cho, *Chem. Eng. J.*, 2014, **242**, 155–161.
- 78 X. Xie, G. Yu, N. Liu, Z. Bao, C. S. Criddle and Y. Cui, *Energy Environ. Sci.*, 2012, **5**, 6862–6866.
- 79 H. Wang, G. Wang, Y. Ling, F. Qian, Y. Song, X. Lu, S. Chen, Y. Tong and Y. Li, *Nanoscale*, 2013, **5**, 10283–10290.
- 80 Y. Qiao, X.-S. Wu, C.-X. Ma, H. He and C. M. Li, *RSC Adv.*, 2014, **4**, 21788–21793.
- 81 C.-. Zhao, W.-J. Wang, D. Sun, X. Wang, J.-R. Zhang and J.-J. Zhu, *Chem. – Euro. J.*, 2014, **20**, 7091–7097.
- 82 Z. He, J. Liu, Y. Qiao, C. M. Li and T. T. Y. Tan, *Nano Lett.*, 2012, **12**, 4738–4741.
- 83 C. K. Chua and M. Pumera, *Chem. Soc. Rev.*, 2014, **43**, 291–312.
- 84 X. Cao, Y. Shi, W. Shi, G. Lu, X. Huang, Q. Yan, Q. Zhang and H. Zhang, *Small*, 2011, **7**, 3163–3168.
- 85 M. Agharkar, S. Kochrekar, S. Hidouri and M. A. Azeez, *Mater. Res. Bull.*, 2014, **59**, 323–328.
- 86 Y. Hou, B. Zhang, Z. Wen, S. Cui, X. Guo, Z. He and J. Chen, *J. Mater. Chem. A*, 2014, **2**, 13795–13800.

